Targeting neurotrophin and nitric oxide signaling to treat spinal cord injury and associated neurogenic bladder overactivity

Youko Ikeda[a,b], Irina Zabbarova[a], Pradeep Tyagi[c], T. Kevin Hitchens[d], Amanda Wolf-Johnston[a], Peter Wipf[e], Anthony Kanai[a,b,*]

[a]University of Pittsburgh, School of Medicine, Department of Medicine, Renal-Electrolyte Division, USA

[b]University of Pittsburgh, School of Medicine, Department of Pharmacology & Chemical Biology, USA

[c]University of Pittsburgh, School of Medicine, Department of Urology, USA

[d]University of Pittsburgh, School of Medicine, Animal Imaging Center, USA

[e]University of Pittsburgh, Dietrich School of Arts and Sciences, Department of Chemistry, USA

Abstract

Purpose or the research: Nearly 300,000 people are affected by spinal cord injury (SCI) with approximately 18,000 new cases annually, according to the National SCI Statistics Center. SCI affects physical mobility and impairs the function of multiple internal organs to cause lower urinary tract (LUT) dysfunctions manifesting as detrusor sphincter dyssynergia (DSD) and neurogenic detrusor overactivity (NDO) with detrimental consequences to the quality of life and increased morbidity. Multiple lines of evidence now support time dependent evolution of the complex SCI pathology which requires a multipronged treatment approach of immediate, specialized care after spinal cord trauma bookended by physical rehabilitation to improve the clinical outcomes. Instead of one size fits all treatment approach, we propose adaptive drug treatment to counter the time dependent evolution of SCI pathology, with three small molecule drugs with distinctive sites of action for the recovery of multiple functions.

Principal results: Our findings demonstrate the improvement in the recovery of hindlimb mobility and bladder function of spinal cord contused mice following administration of small molecules targeting neurotrophin receptors, LM11A-31 and LM22B-10. While LM11A-31 reduced the cell death in the spinal cord, LM22B-10 promoted cell survival and axonal growth. Moreover, the soluble guanylate cyclase (sGC) activator, cinaciguat, enhanced the revascularization of the SCI injury site to promote vessel formation, dilation, and increased perfusion.

*Correspondence to: University of Pittsburgh, School of Medicine, Department of Medicine, A1224 Scaife Hall, 3550 Terrace Street, Pittsburgh, PA, 15261, USA. ajk5@pitt.edu (A. Kanai).

Major conclusions: Our adaptive three drug cocktail targets different stages of SCI and LUTD pathology: neuroprotective effect of LM11A-31 retards the cell death that occurs in the early stages of SCI; and LM22B-10 and cinaciguat promote neural remodeling and reperfusion at later stages to repair spinal cord scarring, DSD and NDO. LM11A-31 and cinaciguat have passed phase I and IIa clinical trials and possess significant potential for accelerated clinical testing in SCI/LUTD patients.

Keywords

Detrusor sphincter dyssynergia (DSD); Neurogenic detrusor overactivity (NDO); p75 neurotrophin receptor (p75^{NTR}); Soluble guanylate cyclase (sGC) activators; Spinal cord injury/contusion (SCI/ SCC); TrkB/C receptors

---

1. Introduction

Neurogenic injury can have severe consequences to multiple physiological functions including mobility and autonomic regulation of internal organs. Lower urinary tract dysfunction (LUTD) is especially prevalent in neurological injury/disease. There are several pharmacological and surgical interventions available that can alleviate the consequences of LUTD, however, they do not restore complete function. Thus, there is still a necessity to expand the knowledge on LUT pathology and identify additional therapeutic targets to improve the functional outcomes. Thus, we posited that multiple, synergistic interventions are required to achieve the highest possible therapeutic results.

Neurotrophins are a family of growth factors that include nerve growth factor (NGF), brain derived neurotrophic factor (BNDF) and neurotrophin-3 and −4 (NT-3/4) (Table 1) that have been attributed to play a key role in the development of LUTD after SCI and modulation of their activity has shown to ameliorate aspects of bladder and urethral sphincter dysfunctions [1,2]. Neurotrophins elicit their actions through the tropomyosin-related kinase (Trk) receptors that are known to activate various cell survival and growth pathways (Fig. 1A). NGF has been primarily associated with the remodeling of sensory innervation and development of the bladder to spinal cord reflex that induces detrusor contraction in response to distention [3]. BNDF has also been implicated in the reflex activity and development of DSD [4]. Previous studies have also implicated the precursor neurotrophins, proneurotrophins, as the initiator of bladder injury following SCI by inducing urothelial layer disruption and apoptosis through its action on the p75 neurotrophin receptor (p75^{NTR}, Fig. 1A) [5,6]. Accordingly, the therapeutic potential of neurotrophin receptors has led to the identification of LM11A-31 and LM22B-10, small molecule modulators of p75^{NTR} and Trk B/C receptors, respectively [7–10]. LM11A-31 selectively acts on p75^{NTR} to inhibit its interaction with proneurotrophins which are elevated in neurodegenerative conditions such as SCI [5,6] and Alzheimer's disease [8,10], thus, LM11A-31 can act as an anti-apoptotic agent. LM22B-10 is a full agonist of Trk B/C receptors and demonstrated to stimulate neural survival and growth in the brain [7].

Vascular dysfunction is also associated with SCI and bladder over-activity [11] which is believed to occur in response to inflammation, oxidative stress and endothelial damage. A hallmark of vascular damage is the impaired responsiveness to nitric oxide (NO•), a key

mediator of vascular smooth muscle relaxation. NO• activates soluble guanylate cyclase (sGC) to generate cyclic guanosine monophosphate (cGMP) that stimulates a multitude of downstream pathways. There are indications that increasing NO•-cGMP signaling can be beneficial in ameliorating SCI induced detrusor overactivity [12]. However, approved agents such as phosphodiesterase (PDE) type 5 inhibitors may have limited efficacy due to decreased NO• bioavailability and/or oxidative inhibition of sGC, essentially preventing cGMP generation. Small molecule sGC activators could circumvent these pathological changes as they can allosterically activate sGC in the absence of its heme prosthetic group and NO• (Fig. 1B) [13]. Studies in SCI rat bladder strips indicate there is decreased responsiveness to NO• donors and PDE5 inhibitors [14], suggestive of sGC dysfunction.

Here we describe investigations of small molecule neurotrophin receptor modulators and a sGC activator to enhance neural sparing and ameliorate LUTD after thoracic level spinal cord contusion injury using a mouse model. The rationale for use of multiple agents is that there are distinct phases in the pathological progression after neurogenic injury and differential treatment is required at each stage. For example, proneurotrophin levels surge immediately following SCI peaking within 24 h [5,6] and trigger apoptotic cascades that have detrimental long-term consequences. Thus, it is postulated that administration of LM11A-31 within this period may prevent these adverse outcomes. Our objective was to determine their potential as therapeutic agents to promote the recovery of mobility and bladder function after SCI.

2. Materials and methods

2.1. Animals

Adult female and male C57Bl/6 mice (8–12 weeks) were purchased from Envigo (Indianapolis, IN) and maintained in a centralized climate-controlled animal facility on a 12 h light/dark cycle (7am to 7pm). Mice were socially housed (four to five mice per cage) in microisolator caging units where food and water were provided ad libitum. Ethical approval was obtained from the Institutional Animal Care and Use Committee for all animal work described.

2.2. Spinal cord contusion (SCC) injury

Mice were anesthetized with isoflurane (5% induction, 2.5% maintenance in 100% O_2) and a laminectomy was performed under sterile surgical conditions between T_8–T_{10} vertebrae to expose the dorsal spinal cord for contusion injury. The musculature around the vertebrae was bluntly dissected and the vertebrae column was secured using a customized holder before removal of the lamina. The exposed cord was subjected to a severe contusion injury (Fig. 1C–D, 75 kilodyne) using the IH-0400 Infinite Horizon Impactor (Precision Systems and Instrumentation, LLC). Immediately following contusion, the exposed cord was covered with hemostatic sponge and in a select cohort, an osmotic pump (ALZET #1004) with LM22B-10 (5 mg/kg/day, Tocris, Minneapolis, MN) or vehicle was placed subcutaneously on the flank of the mouse. The muscle and skin layers were sutured separately, and recovery observed for two hours after surgery. Mice were monitored twice daily during the first week after surgery, provided prophylactic antibiotic, ampicillin (100 mg/kg twice daily for seven

days) and analgesic, ketoprofen (3 mg/kg, twice daily for three days) and manual bladder expression performed until reflex voiding was established (approximately 5 to 7 days after injury). Sham animals were subjected to the laminectomy surgery without contusion injury.

2.3. Hindlimb locomotion assessments

Recovery of hindlimb function was assessed at one, three, seven, 14, 28, 35 and 42 days following contusion using the Basso Mouse Scale (BMS) method [15] based on observations of leg movement, weight bearing, plantar stepping motion, coordination and trunk stability. Mice were evaluated using the BMS scoring sheet by at least two assessors at each time point with evaluation performed independently. The score sheet was used to derive the primary BMS score (0–9) and a sub-score (0–11) which was used to further refine differences in stepping activity.

2.4. Drugs

Cinaciguat (Tocris, Minneapolis, MN) was dissolved in DMSO, suspended in 1% methylcellulose and administered by daily gavage (10 mg/kg). LM11A-31 (synthesized in house) was dissolved in sterile water and administered by daily gavage (100 mg/kg). LM22B-10 (Tocris) was dissolved in 50% DMSO and 50% sterile saline and filled into osmotic pumps under aseptic conditions.

2.5. Fluorescent bead vascular labeling

Mice were anesthetized with isoflurane and a PE10 catheter inserted into the jugular vein for perfusion with 1xPBS with 500 U heparin using a syringe pump at 10 μl/min followed by solution with fluorescent microbeads (F8787, Thermofisher, 0.02 μm) for 10–15 min. Animals were sacrificed immediately after perfusion, their spinal cords removed and fixed in 4% paraformaldehyde (PFA) for 48 h followed by incubation in graded sucrose. Tissues were frozen in optimal cutting temperature medium and sectioned 100–400 μm thick on a cryostat. Sections were cleared using the ClearT2 method [16], mounted onto slides, and imaged using confocal microscopy (FV3000, Olympus, Tokyo, JP).

2.6. Mitochondrial respiration assessment

Mitochondria were isolated from control, SCC and SCC treated with cinaciguat C57Bl/6 mouse spinal cords as described previously [17] with modifications. After deep anesthesia with isoflurane (2%–5%), the spinal cord ($\approx$60 mg) was isolated by extrusion [18] and placed in a mitochondrial solution containing 5 mM HEPES, 125 mM KCl, 2 mM monobasic KH_2PO_4, 20 μM EDTA, 5 mM $MgCl_2$ and 0.2 mg/ml BSA, adjusted to pH 7.4 with 100 mM KOH. The spinal cord was minced by a McIlwain motorized tissue chopper (Brinkmann) set to chop at a interval, placed in 10 ml of mitochondrial solution and homogenized by a few passes with a motorized (75 rpm) Teflon pestle. The homogenate was spun at $1000 \times g$ for 10 min. The supernatant was again spun at $10,000 \times g$ for 10 min to obtain a second pellet containing the mitochondria. Pellets were resuspended in 100 μl of mitochondrial solution, and 25 μl of the suspension placed in a gas-tight vessel containing a Clark-type oxygen microelectrode (MI-730/OM-4; Microelectrodes, Londonderry, NH) to measure the state 3 (succinate + ADP) and state 4 (succinate alone) respiratory rates. The

electrode was calibrated considering the total amount of dissolved O_2 in aqueous solution after equilibration with air at 36 °C to be 215 μM [19] and zeroed with sodium dithionite. The respiratory control ratio (RCR), a measure of the "tightness of coupling" between electron transport and oxidative phosphorylation, was determined from the ratio of state 3 to state 4 rates of respiration. A RCR of 2–4 is considered good for complex II substrates [20].

2.7.   Magnetic resonance imaging (MRI)/Diffusion tensor imaging (DTI) of isolated spinal cords

PFA fixed mouse spinal cords were dissected to 20 mm long lumbar-cervical segments and placed in a 5 mm glass NMR tube containing perfluorocarbon oil (Fluorinert FC-40, Sigma-Aldrich, St Louis, MO) as a magnetic susceptibility matching fluid. A glass Shigemi NMR tube plunger was inserted to secure the tissue in place. MRI was performed using a Bruker AV3HD 11.7 Tesla/89 mm vertical-bore microimaging system equipped with a 16-channel shim insert and Micro2.5 gradient set with a maximum gradient of 1500 mT/m and data collected using a 5 mm RF resonator and ParaVision 6.0.1 (Bruker Biospin, Billerical MA). Sample temperature was maintained at 22 °C using a variable temperature module. Following pilot scans, the field homogeneity was optimized with field map shimming. Anatomical MRI scans were acquired using a three dimensional T2-weighted RARE TR/TE 1000/36 ms, $15.6 \times 5 \times 5$ mm FOV at 100 mm isotropic resolution. Diffusion Tensor Imaging were collected with a spin-echo sequence TR/TE = 2000/26 ms, with Stejskal–Tanner diffusion scheme with D/d = 15/6 ms, two shells (b=1000, 2000 s/mm ^{2}), a total of 18 diffusion encoding directions with two B0 images, fifty 0.3 mm slices, 5 mm FOV, 64×64 matrix and 8 averages. Diffusion tensor images were reconstructed with DSI Studio software. Regions of Interest (ROIs) were manually drawn in the white matter on each image slice and plots of DTI scalar measures, Fractional Anisotropy (FA), Mean Diffusivity (MD), Axial Diffusivity (AD) and Radial Diffusivity (RD), will be generated vs. slice position.

2.8.   Histology and immunofluorescent analysis

At the experimental endpoints, mice were placed under deep isoflurane anesthesia and a thoracotomy was performed. The mouse was immediately transcardially perfused with 1x tris buffered saline (TBS) followed by 10% neutral buffered formalin (NBF). Spinal cord segments for histology were isolated and placed in 10% NBF overnight followed by 30% sucrose for cryopreservation. Segments were sectioned 20 μm thick on a cryostat and stored at −30 °C until processed for immunofluorescence or staining. Collagen content in the spinal lesion was assessed by Van Gieson staining (MilliporeSigma, Burlington, MA) with omission of hematoxylin/elastin stain. Immunofluorescent detection was performed as previously described [21] and antibodies utilized are summarized Table A.1 in the Appendix. Collagen content and spinal cord lesion area quantification was performed with FIJI ImageJ software and averaged from three sequential sections for each animal.

2.9.   Statistical analysis

Continuous measures were expressed as mean ± standard error of the mean (SEM). Between group differences were assessed by one-way ANOVA with Tukey's post-hoc multiple comparison analysis (Prism 9, GraphPad) and significance was determined as p<0.05.

3. Theory

We hypothesize that temporal changes in the levels of paracrine signaling messengers at the injury site in the spinal cord drive the initiation and the spread of neurodegeneration following SCI. There is an initial surge in the proneurotrophins that are released almost immediately after the injury to activate apoptotic signaling. Proneurotrophins levels start to decrease within 24 h after which there is partial recovery. However, altered neurotrophin activity over time is further compounded by the overproduction of cerebrospinal fluid which hydrostatically opposes neovascularization and the resulting deprivation of oxygen at the injury site inhibits neuroregeneration. Our proposed adaptive multipronged action of three drugs is predicted on time dependent changes in paracrine signaling for achieving synergistic action on multiple signaling mechanisms to support functional recovery and tissue repair. We propose targeting three distinct receptor pathways; the p75^{NTR}, TrkB/C and NO•-cGMP pathways using novel pharmacological agents to inhibit neuronal and urothelial apoptosis, to promote growth/survival and to support angiogenesis/repair for improved functional recovery.

4. Results

4.1. LM11A-31 promotes functional recovery by sparing the nerve fiber tracks visualized with MRI and diffusion tensor imaging (DTI)

DTI (Fig. 2) relies on the orientation of directional diffusion of water molecules within the tissues. Inside the spinal cord, water diffusion in white matter axons is limited by the cell membrane and diffusion mainly occurs parallel to the white matter tracts with less diffusion in the perpendicular direction. SCI damages the cell membrane to cause unrestricted perpendicular water diffusion radial to the site of injury [22]. Accordingly, DTI allows the visualization of nerve tracts over the entire spinal cord in a more time efficient and accurate manner. DTI was performed on the thoracic region of non-injured (Fig. 2A), sham operated male (Fig. 2B), SCC male (Fig. 2C) and SCC male mice given LM11A-31 for the first 7 days after surgery, starting within three hours after surgery (Fig. 2D). Tissues were collected 60 days after surgery. These studies demonstrate the feasibility of MRI to distinguish the injury and repair of white matter tracts in the mouse spinal cord for discerning the neuroprotection by LM11A-31 which engenders greater tissue sparing compared to vehicle SCC mice, as shown by MR images, diffusivity measurements and fiber tracking (Fig. 2E and F). Hindlimb locomotion assessments correlated with MR imaging showing significant improvement with LM11A-31 compared to the vehicle treated mice at 14 days post SCI (Fig. 2G).

4.2. LM22B-10 improves the recovery of hindlimb function and ameliorates neurogenic bladder dysfunction

Female C57Bl/6 mice were subjected to severe contusion injury (Fig. 1C–D) and at the time of injury also implanted with osmotic pumps to deliver the TrkB/C selective agonist, LM22B-10 (5 mg/kg/day) [7] or vehicle over a 4-week period. Assessment of hindlimb movement showed that the LM22B-10 treated cohort had significantly better hindlimb recovery at 28, 35 and 42 days after surgery (Fig. 3A–B). Recovery of hindlimb

movement correlated with an improved LUT function as demonstrated in decerebrate filling cystometrogram (CMG) and EUS electromyogram (EMG) recordings (Fig. 3C–E). LM22B-10 treated SCC mice had less frequent non-voiding contractions (NVCs) and exhibition of DSD, and improved voiding efficiency (n 4). The decreased time windows to the right of the traces demonstrate the increase in tonic activity of the EUS in SCC animal (Fig. 3D) indicative of DSD. The EMG trace in Fig. 3E demonstrates that the EUS tonic activity decreases as does the bladder pressure indicative of a small void occurring.

4.3. LM22B-10 decreases the spinal cord lesion area but not collagen content

To assess whether LM22B-10 was promoting recovery *via* enhanced survival of neural tissue, we examined histological sections of spinal cord segments around the lesion. Longitudinal sections (rostral to caudal) were obtained and the localization of glial fibrillary acidic protein (GFAP, marker for activated astrocytes/glia—green) and 5-hydroxytrypamine (5-HT, transmitter in interneurons—red) was examined by immunofluorescence (Fig. 4A–C). Chronic SCC resulted in a significant disruption of the spinal cord architecture (Fig. 4B). In SCC mice, a large lesion extended along the dorsal aspect, delineated by GFAP positive cells. LM22B-10 treated SCC mice showed a reduction in the overall lesion area and frequently exhibited smaller lesions scattered around the injury epicenter (Fig. 4C). Comparable sections examined with Van Gieson stain without hematoxylin revealed that collagen infiltration at the spinal cord scar was not significantly different between vehicle and LM22B-10 cohorts (Fig. 4D–E).

4.4. Cinaciguat improves mitochondrial respiration in SCC mice

The neuro protective effect of cinaciguat in the spinal cord was assessed by measuring the respiration of mitochondria (Fig. 5) isolated from spinal cords of female sham, SCC, and SCC mice given cinaciguat (10 mg/kg/day/7days). These experiments showed that a decrease in RCR following SCC was normalized by cinaciguat (Table 2). Improved RCR values with cinaciguat treatment correlated with the high density of blood vessels around the spinal cord lesion (Fig. 5D–F).

5. Discussion

These findings provide empirical support for targeting three distinct signaling pathways using novel pharmacological agents to inhibit apoptosis and promote growth/survival while also supporting angio-genesis/repair at different time points following SCI. We evaluated morphological changes in the spinal cord using MRI, microbead infusion with confocal imaging and histological techniques, and assessed functional recovery of urinary bladder activity using cystometry and hindlimb locomotion. These assessments were supported by molecular techniques including protein analysis for biomarkers and mitochondrial respiration measurements of spinal cord tissues.

LM11A-31 has been shown to selectively bind with p75^{NTR} to inhibit proneurotrophin induced apoptosis [8]. We have previously reported on the efficacy of LM11A-31 on the amelioration of LUTD in SCI mice with complete spinal cord transections [5,6] where it is thought to act on the urothelium and nerves innervating the urinary bladder. In

this study, we demonstrated administration of LM11A-31 within three hours after SCI and continued daily for seven days resulted in improved hindlimb recovery and nerve track sparing (Fig. 2). Irrespective of the spinal level of injury, SCI leads to rewiring within the lumbosacral spinal cord to establish a reflex between bladder sensory nerves and preganglionic parasympathetic nuclei and/or EUS motoneurons [3]. This is largely driven by the initial surge of proneurotrophins in the bladder which disrupts urothelial integrity, initiates neural degeneration and promotes inflammation to cause LUTD. Since the abrupt rise in proneurotrophins subsides quickly after peaking within 24 h after SCI [6], we reasoned that the administration of LM11A-31 should occur as soon as possible after stabilization of the patient as a prophylactic intervention for slowing down the neurodegeneration by limiting the proneurotrophin induced apoptotic cascade.

In silico analysis of LM11A-31 congeners for affinity to neurotrophin receptors [7] led to the identification of LM22B-10 as a TrkB/C selective agonist for promoting the survival and growth of hippocampal neurons [9]. Here, we demonstrate that LM22B-10 improved mobility and ameliorated LUTD in SCI mice when given up to 28 days after injury. Our findings are supported by a previous report using the partial TrkB/C agonist, LM22A-4, which also reduced the secondary tissue injury in SCI models [23]. It is possible that further improvement could have been achieved if treatment was continued past 28 days, which would require further investigation. We propose LM22B-10 could be used as a trophic support agent for early to chronic stages of SCI. Furthermore, we did not observe increased signs of pain or distress with LM22B-10 treatment as there was no significant difference in post-surgical weight loss compared to vehicle cohort up to 42 days after SCI (not shown). Therefore, we do not anticipate LM22B-10 treatment would aggravate neuropathic pain, a potential complication with SCI.

Cinaciguat is a potent sGC activator with vasodilatory effects and was initially investigated as a treatment for acute heart failure [24]. The unique feature of sGC activators is their ability to induce cGMP generation when the sGC heme moiety is oxidized or absent and the NO•-signaling pathway is compromised. The binding of sGC heme is regulated by its redox state and only attaches when the heme is in the reduced state. This is especially important in SCI which is accompanied by systemic inflammation and chronic oxidative stress that would promote heme oxidation and inactivation of sGC. Our data show SCC resulted in significant alterations in mitochondrial RCR in spinal cord tissue which was normalized by the treatment with cinaciguat. Our data suggest that angiogenesis around the spinal cord lesion occurs slowly, leading to chronic ischemia and cellular metabolic dysfunction. sGC activators such as cinaciguat can promote angiogenesis [25] which in this case is functionally reflected as improved RCR values. Further, we propose that the efficacy of cinaciguat would be highest in damaged tissues where sGC heme oxidation/loss occur. This is supported by the limited effect of the PDE5 inhibitor, sildenafil on the spinal cord revascularization and functional recovery after SCI [26], presumably due to oxidative stress induced sGC inactivation.

A major focus of this study was to support the translational potential of the proposed drugs for enhancing the functional recovery following SCI. There are currently no drugs approved for this purpose, likely due to the complexity of SCI pathology that progresses over time and

therefore not amenable to a one drug approach. Thus, we reasoned that repair of the injured spinal cord and functional recovery requires time-bound targeting of multiple signaling pathways at critical time points. The proposed route and dosing for each of the drugs were based upon their absorption, distribution, metabolism, and excretion profiles. LM11A-31 is a water-soluble drug, oral dosing of 50 mg/kg by gavage achieved peak brain concentration in mice within approximately 30 min and its uptake into the CNS is proposed to involve active transport [10]. LM22B-10 and cinaciguat are poorly water-soluble drugs that were solvated in DMSO and administered by an osmotic pump or gavage. All three drugs are excreted by hepatic clearance in feces.

6. Conclusion

Our data support there are multiple pathways that can be manipulated to improve functional outcomes following neurogenic injury. Further investigations are required into combination treatments that provide neurotrophic support and revascularization with the aim to improve recovery of mobility and bladder functions.

Funding sources

Appendix

(See Table A.1.)

Table A.1

List of antibodies.

| Target	Dilution	Host	Manufacturer/lot number
glial fibrillary acidic protein (GFAP)	1:1,000	Rat	Thermofisher,
5-HT	1:1,000	Rabbit	Immunostar
anti-rat alexfluor-488	1:500	Donkey	Thermofisher
anti-rabbit alexfluor-594	1:500	Donkey	Thermofisher

References

[1]. Seki S, et al. , Immunoneutralization of nerve growth factor in lumbosacral spinal cord reduces bladder hyperreflexia in spinal cord injured rats, J. Urol 168 (5) (2002) 2269–2274. [PubMed: 12394773]

[2]. Wada N, et al. , Therapeutic effects of inhibition of brain-derived neurotrophic factor on voiding dysfunction in mice with spinal cord injury, Am. J. Physiol. Renal. Physiol 317 (5) (2019) F1305–F1310. [PubMed: 31566429]

[3]. de Groat WC, Yoshimura N, Plasticity in reflex pathways to the lower urinary tract following spinal cord injury, Exp. Neurol 235 (1) (2012) 123–132. [PubMed: 21596038]

[4]. Frias B, et al. , The role of brain-derived neurotrophic factor (BDNF) in the development of neurogenic detrusor overactivity (NDO), J. Neurosci 35 (5) (2015) 2146–2160. [PubMed: 25653370]

[5]. Ryu JC, et al. , Role of proNGF/p75 signaling in bladder dysfunction after spinal cord injury, J. Clin. Invest 128 (5) (2018) 1772–1786. [PubMed: 29584618]

[6]. Zabbarova IV, et al. , Targeting p75 neurotrophin receptors ameliorates spinal cord injury-induced detrusor sphincter dyssynergia in mice, Neurourol. Urodyn 37 (8) (2018) 2452–2461. [PubMed: 29806700]

[7]. Yang T, et al. , A small molecule TrkB/TrkC neurotrophin receptor co-activator with distinctive effects on neuronal survival and process outgrowth, Neuropharmacology 110 (Pt A) (2016) 343–361. [PubMed: 27334657]

[8]. Massa SM, et al. , Small, nonpeptide p75NTR ligands induce survival signaling and inhibit proNGF-induced death, J. Neurosci 26 (20) (2006) 5288–5300. [PubMed: 16707781]

[9]. Gonzalez S, et al. , Small molecule modulation of TrkB and TrkC neurotrophin receptors prevents cholinergic neuron atrophy in an Alzheimer's disease mouse model at an advanced pathological stage, Neurobiol. Dis 162 (2022) 105563. [PubMed: 34838668]

[10]. Knowles JK, et al. , Small molecule p75NTR ligand prevents cognitive deficits and neurite degeneration in an Alzheimer's mouse model, Neurobiol. Aging 34 (8) (2013) 2052–2063. [PubMed: 23545424]

[11]. Yao C, Cao X, Yu B, Revascularization after traumatic spinal cord injury, Front. Physiol 12 (2021) 631500. [PubMed: 33995118]

[12]. Sasatomi K, et al. , Nitric oxide-mediated suppression of detrusor overactivity by arginase inhibitor in rats with chronic spinal cord injury, Urology 72 (3) (2008) 696–700. [PubMed: 18358516]

[13]. Schmidt HH, Schmidt PM, Stasch JP, NO- and haem-independent soluble guanylate cyclase activators, Handb. Exp. Pharmacol (191) (2009) 309–339.

[14]. Artim DE, et al. , Developmental and spinal cord injury-induced changes in nitric oxide-mediated inhibition in rat urinary bladder, Neurourol. Urodyn 30 (8) (2011) 1666–1674. [PubMed: 21717503]

[15]. Basso DM, et al. , Basso mouse scale for locomotion detects differences in recovery after spinal cord injury in five common mouse strains, J. Neurotrauma 23 (5) (2006) 635–659. [PubMed: 16689667]

[16]. Kuwajima T, et al. , ClearT: a detergent- and solvent-free clearing method for neuronal and non-neuronal tissue, Development 140 (6) (2013) 1364–1368. [PubMed: 23444362]

[17]. Kanai AJ, et al. , Identification of a neuronal nitric oxide synthase in isolated cardiac mitochondria using electrochemical detection, Proc. Natl. Acad. Sci. USA 98 (24) (2001) 14126–14131. [PubMed: 11717466]

[18]. Richner M, et al. , Hydraulic extrusion of the spinal cord and isolation of dorsal root ganglia in rodents, J. Vis. Exp (119) (2017).

[19]. Wise RR, Naylor AW, Calibration and use of a Clark-type oxygen electrode from 5 to 45 degrees C, Anal. Biochem 146 (1) (1985) 260–264. [PubMed: 3993936]

[20]. Silva AM, Oliveira PJ, Evaluation of respiration with Clark-type electrode in isolated mitochondria and permeabilized animal cells, Methods Mol. Biol 1782 (2018) 7–29.

[21]. Ikeda Y, et al. , Relaxin-2 therapy reverses radiation-induced fibrosis and restores bladder function in mice, Neurourol. Urodyn 37 (8) (2018) 2441–2451. [PubMed: 29806709]

[22]. Zaninovich OA, et al. , The role of diffusion tensor imaging in the diagnosis, prognosis, and assessment of recovery and treatment of spinal cord injury: a systematic review, Neurosurg. Focus 46 (3) (2019) E7.

[23]. Yu G, Wang W, Protective effects of LM22a-4 on injured spinal cord nerves, Int. J. Clin. Exp. Pathol 8 (6) (2015) 6526–6532. [PubMed: 26261531]

[24]. Breitenstein S, et al. , Novel sGC stimulators and sGC activators for the treatment of heart failure, Handb.Exp. Pharmacol 243 (2017) 225–247. [PubMed: 27900610]

[25]. Pyriochou A, et al. , Soluble guanylyl cyclase activation promotes angiogenesis, J. Pharmacol. Exp. Ther 319 (2) (2006) 663–671. [PubMed: 16940434]

[26]. Myers SA, et al. , Sildenafil improves epicenter vascular perfusion but not hindlimb functional recovery after contusive spinal cord injury in mice, J. Neurotrauma 29 (3) (2012) 528–538. [PubMed: 21970599]

Table 1. neurotrophin receptors and known ligands

Receptor	Ligand
p75^{NTR}	pro-NGF, -BDNF, -NT3, -NT4
TrkA	NGF
TrkB	BDNF/NT-4
TrkC	NT-3

30 kDy (mild SCC); 50 kDy (moderate SCC); 70 kDy (severe SCC)
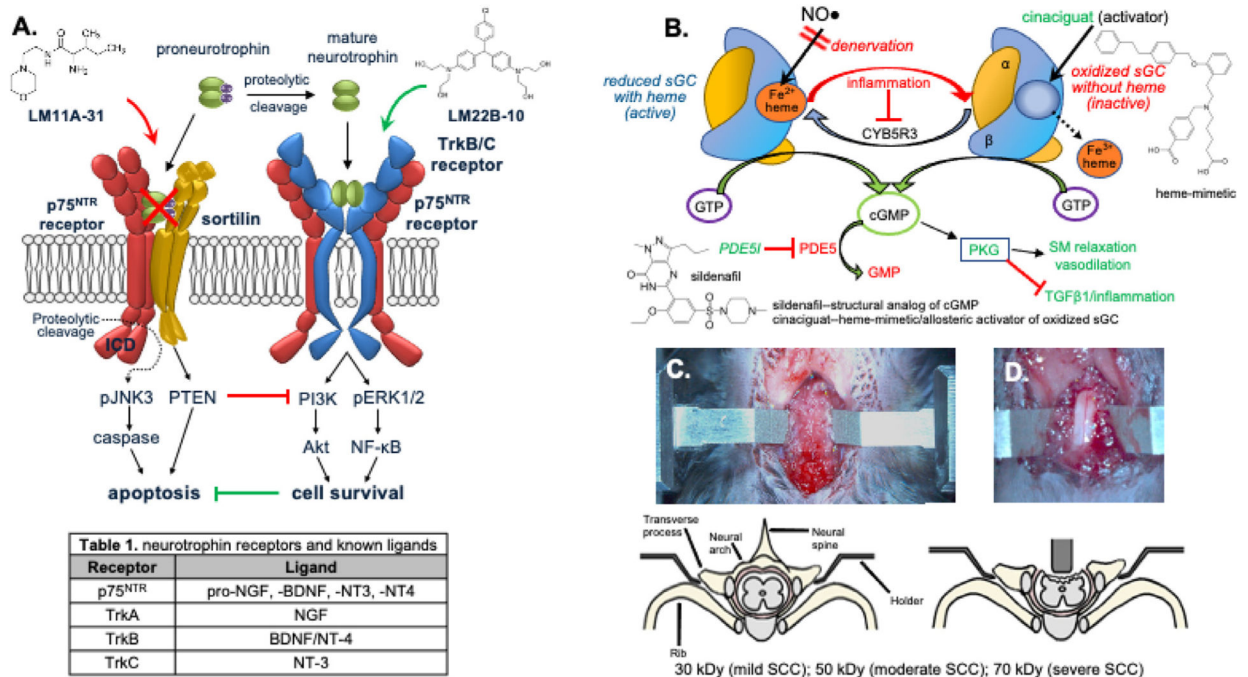
Fig. 1. p75^{NTR} and sGC-cGMP signaling pathways.
A. While the p75^{NTR}-sortilin complex preferentially binds with proNGF/proBDNF to activate apoptotic signaling cascades and p75^{NTR}-Trk complex binds with mature neurotrophins to activate cell survival. LM11A-31 targets the p75^{NTR}-sortilin complex to prevent the activation of apoptotic cascades. Table 1. Neurotrophin receptors and their ligands. B. Since cGMP production by NO• requires a reduced heme (Fe^{2+}) in the active site of sGC, reduction of sGC heme by CYB5R3 sensitizes it to NO•. The unresponsiveness of heme free sGC to NO• in pathology is reverted by sGC activators are heme mimetics, which do not require NO• or heme to stimulate cGMP production. Images of male mouse T$_8$–T$_9$ spinal cord segments C. before and D. after laminectomy. Fig. 1A and Table 1 are adapted from reference [6] and Fig. 1B is adapted from I. Zabbarova et al., J Pathol. 2022 Apr; 256(4):442–454
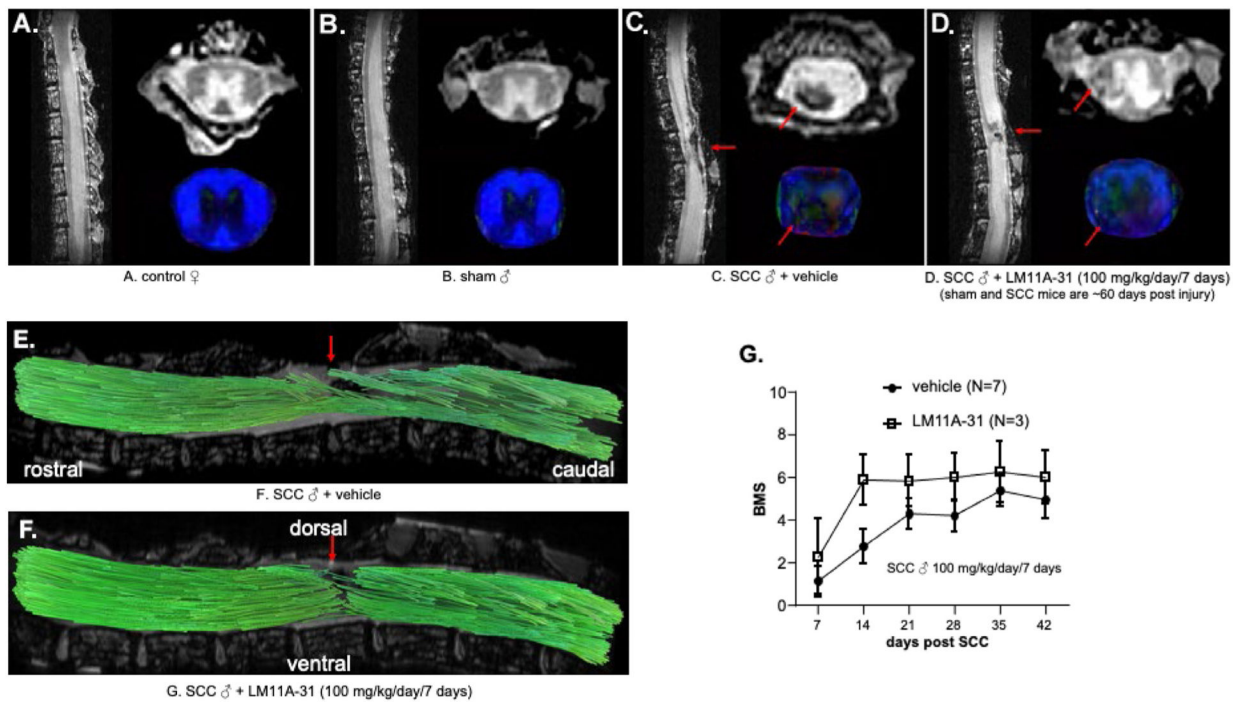
Fig. 2. Magnetic resonance imaging (MRI) of spinal cords and plots of diffusion tensor imaging (DTI) vs. position.
Images from: A. control, B. sham, C. contused, and D. LM11A-31 treated mice. The panels display T_2-weighted images in the sagittal plane (left), axial plane (top right), and directionally encoded color (DEC) maps, bottom right. MR images are grayscale and the hues in DEC maps index the orientation of fractional anisotropy (FA). For intact cords (panels A–B), anterior/posterior FA is displayed by blue; for injured cords (C–D), changes in FA are displayed by green (dorsal/ventral) and red (left/right) at the lesion (red arrows). The integrity of the gray matter (central region of the cord) in D compared to C demonstrates that LM11A-31 limits tissue degeneration. DTI data is from 15 mm fields of view (FOV) in 0.3 mm slices centered on the injury site. Fiber tracking of E. vehicle and F. LM11A-31 treated contused mouse cords using data from C and D, respectively; the red arrows to the sites of injury. G. Basso mouse score (BMS) for male SCC mice following daily gavage with LM11A-31 (100 mg/kg) or vehicle.
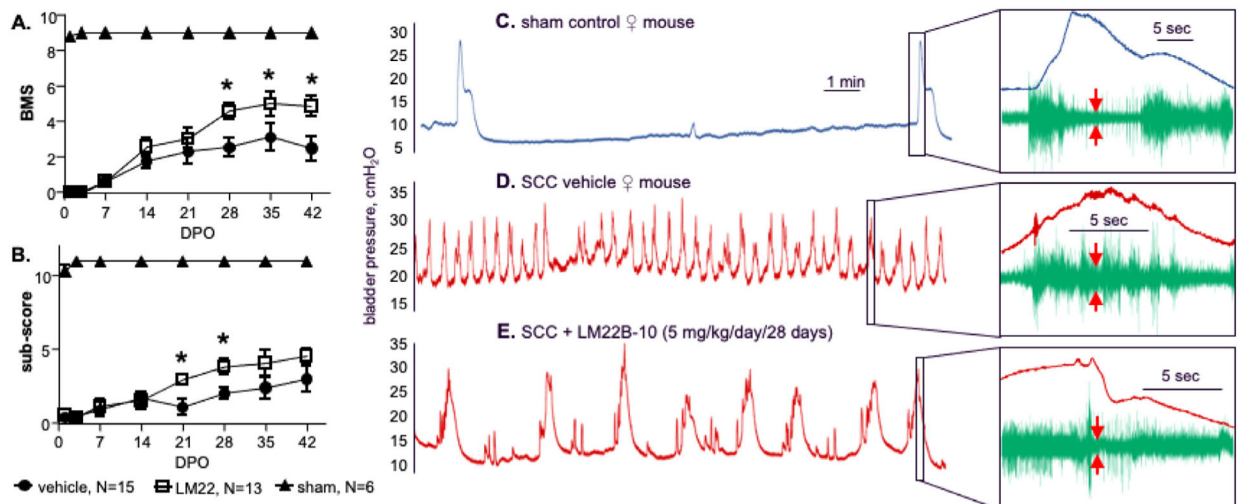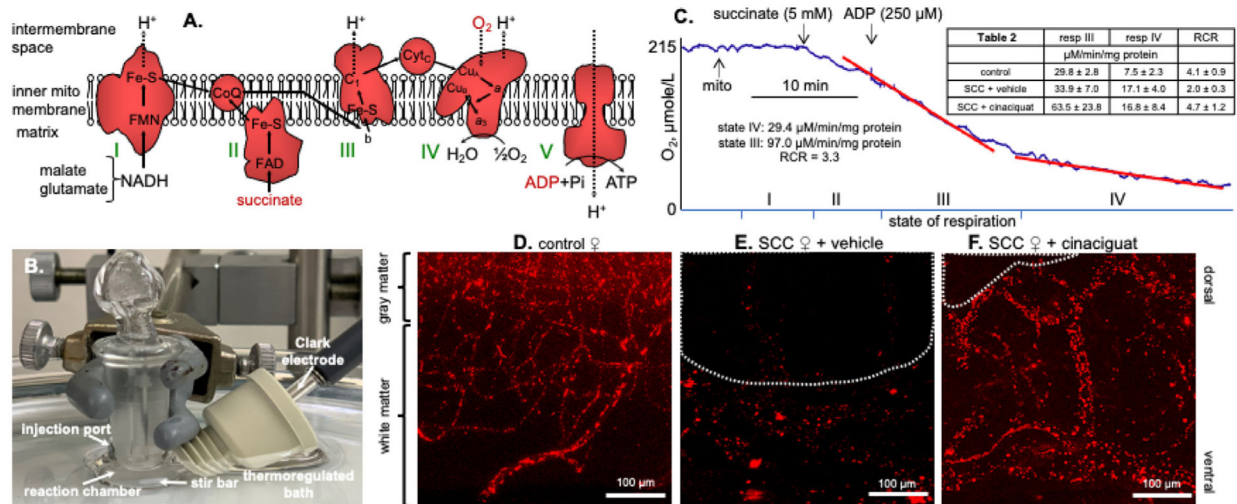
Fig. 3. Improved hindlimb locomotion recovery and LUT function in LM22B-10 treated SCC mice.

A. Basso hindlimb locomotion scores and B. sub-scores from SCC with vehicle, SCC with LM22B-10 treatment and sham female mice between 3 to 42 days post operation (DPO). Scoring was performed by two trained assessors blinded to the test group designation independently. Mean ±SEM, *= p<0.05, LM22B-10 *vs.* vehicle SCC, one-way ANOVA with Tukey's multiple comparison test. Decerebrate CMG–EUS–EMG recordings from C. sham female, D. SCC with vehicle and E. SCC with LM22B-10 treatment. Breakout boxes show expanded time bases with EUS-EMG traces demonstrating changes in tonic firing during bladder contractions. Reduction in EUS tonic firing during bladder contraction facilitates urine outflow.

GFAP (green), 5-HT (red), and DAPI (blue)
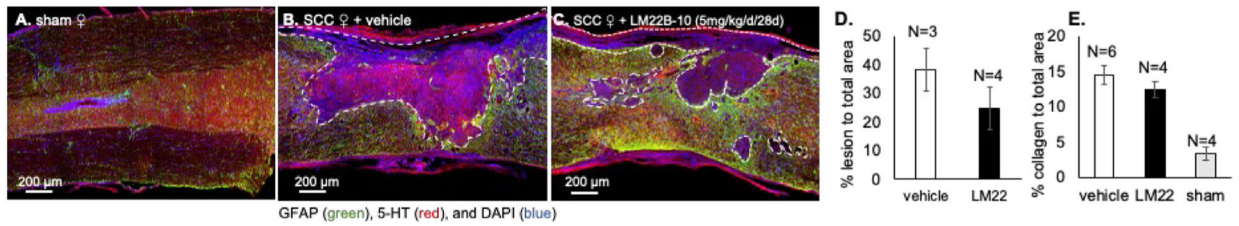
Fig. 4. LM22B-10 reduces total spinal cord lesion area but not collagen deposition.
Immunofluorescent image of T_8–T_9 spinal cord section labeled with glial fibrillary acidic protein (GFAP, green), 5-hydroxytryptophan (5-HT, red) and DAPI (blue) from A. a sham female mouse B. SCC female mouse with vehicle treatment. C. SCC female mouse treated with LM22B-10 (5 mg/kg/day/28days). D. Bar chart of % lesion area *vs.* total measurement area, determined from an area 2 mm on either side of the lesion epicenter. E. Bar chart of % collagen in T_8–T_9 spinal cord sections from SCC vehicle, SCC LM22B-10 treated and sham female mice. Comparable sections were processed with Van Gieson stain omitting hematoxylin. Percentage area of collagen (not shown) was calculated *vs.* total measured area.

Table 2.

Table 2	resp III	resp IV	RCR
	μM/min/mg protein		
control	29.8 ± 2.8	7.5 ± 2.3	4.1 ± 0.9
SCC + vehicle	33.9 ± 7.0	17.1 ± 4.0	2.0 ± 0.3
SCC + cinaciguat	63.5 ± 23.8	16.8 ± 8.4	4.7 ± 1.2

Fig. 5. Spinal cord mitochondrial respiration and blood vessel density.
A. The five mitochondrial complexes located near the inner membrane. B. The glass chamber used for mitochondrial respiration measurements positioned in a thermoregulated water bath C. Typical oxygen consumption measurement by a Clark microelectrode depicting the four states of mitochondrial respiration: I, respiration with internal substrates; II, respiration stimulated by additional substrates (succinate for complex II); III, the state induced by addition of high (100–300 μM) concentrations of ADP; state IV is obtained when ADP is depleted by phosphorylation to ATP. The respiratory control ratio (RCR) is a measure of the tightness in mitochondrial coupling which is determined from the ratio of state 3 to state 4 respiration. A RCR of 3 and above with succinate as substrate is considered tightly coupled, while 1–2 indicates damaged mitochondria. Table 2. Respiration rates and RCRs of spinal cord mitochondria isolated from control, contused, and contused mice treated with cinaciguat(10 mg/kg/day/7 days). D. Confocal image of a longitudinal spinal cord section at the level of injury epicenter from a control female mouse following I.V. infusion of 0.02 μm red fluorescent microbeads. E. SCC female gavaged daily with methylcellulose (N=2). White dotted line delineates the lesion area. F. SCC female given daily cinaciguat (10 mg/kg/day, N=2).